Cytotherapy 28 (2026) 102141

Contents lists available at ScienceDirect

FULL-LENGTH ARTICLE

CYTOTHERAPY

journal homepage: www.isct-cytotherapy.org

International Society ISCT Cell & Gene Therapy®

Immunotherapy (CAR-T, T Reg, NK Cells etc.)

Targeting intratumoral heterogeneity in pancreatic cancer with sequential TIL infusions

Lucas C.M. Arruda[1,2,*], Julia Karbach[3,*], Dragan Kiselicki[3], Evgueni Sinelnikov[4], Dirk Gustavus[4], Hans Hoffmeister[4], Akin Atmaca[3], Elke Jäger[3,]**

[1] Department of Medicine Huddinge, Karolinska Institutet, Stockholm, Sweden
[2] CuraCell, Solna, Sweden
[3] Department of Oncology and Hematology, Krankenhaus Nordwest, Frankfurt, Germany
[4] Zellwerk GmbH, Eichstaedt, Germany
**Correspondence: Elke Jäger, MD, Department of Oncology and Hematology, Krankenhaus Nordwest, Steinbacher Hohl 2-26, 60488, Frankfurt am Main, Germany. *E-mail address:* ej200161@aol.com (E. Jäger).
[*]These authors contributed equally and shared first authorship.

A B S T R A C T

Adoptive transfer of tumor-infiltrating lymphocytes (TIL) is effective in melanoma and selected solid tumors, but its potential in pancreatic ductal adenocarcinoma (PDAC) remains largely unexplored. We report a 39-year-old male with metastatic PDAC involving lung, peritoneal, liver, and lymph node who received three sequential infusions of TIL expanded *ex vivo* with IL-2/IL-15/IL-21 from a lung metastasis. Each infusion followed low-dose lymphodepletion and IL-2 support. The patient achieved stable disease after the first infusion and a partial response after the second along with reductions in serum CA19-9. Genome sequencing revealed substantial inter-tumoral heterogeneity, with mutations in *ITGB2, C1QTNF3, CDK9, TMEM200C, FHOD1* and *ZZZ3* impacting TIL infiltration and clinical response. RNA-seq showed that responding lesions were enriched for inflammatory and tumor-specific programs, displayed enrichment of T-cell activation transcripts and had reduced infiltration of cancer-associated fibroblasts. TCR sequencing confirmed the robust infiltration of TIL-derived CD8+ clonotypes, while functional assays demonstrated a polyclonal recognition of patient-derived somatic mutations and cytotoxicity against autologous tumor lines. Single-cell TCR mapping further validated the dominance of tumor-specific CD8+ clonotypes in responding lesions. This case demonstrates the feasibility and immunological activity of TIL therapy in PDAC, while underscoring the impact of spatial tumor heterogeneity on therapeutic outcomes.

Key Words: cytotoxic T-cells, IL-2, IL-15, IL-21, pancreatic ductal adenocarcinoma, tumor-infiltrating lymphocytes.

Introduction

Pancreatic ductal adenocarcinoma (PDAC) remains one of the most lethal malignancies despite advances in surgery, chemotherapy and radiotherapy, with median survival of 4 months and a 5-year survival of 13% [1]. The poor prognosis is primarily driven by late diagnosis due to its asymptomatic onset, rapid metastatic progression, and profound resistance to systemic therapies [2]. Immunotherapy has transformed the treatment landscape of several cancers, including melanoma and lung cancer, but progress in PDAC remains limited due to its immunosuppressive tumor microenvironment (TME) [3,4].

The complex interplay between malignant cells, infiltrating immune cells, and cancer-associated fibroblasts (CAFs) results in profound immune dysfunction and restricts infiltration of key anti-tumor populations such as $CD8^+$ T-cells, natural-killer cells, and of pro-inflammatory M1 macrophages, N1 neutrophils, and Th1 cells [4]. The abundance of suppressive cells aligned with the deficiency of anti-tumor immunity has rendered PDAC largely unresponsive to immune checkpoint blockade (ICB). Despite successful in other tumors, anti-CTLA-4 [5] and anti−PD-L1 [6] therapies have shown limited success in PDAC, both as monotherapies and in combination regimens [7]. Similarly, attempts to modulate the TME and enhance anti-tumor immune responses have also been unsuccessful. Pegilodecakin, a pegylated recombinant human IL-10, combined with FOLFOX did not improve outcomes in advanced gemcitabine-refractory PDAC [8], and vaccination with Algenpantucel-L failed to confer a survival benefit in patients with borderline resectable or locally advanced unresectable PDAC receiving standard neoadjuvant chemotherapy and chemoradiation [9]. These shortcomings highlight the necessity of strategies that can overcome immune exclusion and re-engage tumor-reactive lymphocytes.

The poor responses rates to immunotherapy are partially attributed to its low mutation burden, which generates few tumor-specific neoantigens and limits T-cell infiltration [10]. Nevertheless, neoantigen quality has been linked to long-term survival in PDAC, indicating

https://doi.org/10.1016/j.jcyt.2026.102141

that most patients harbor neoantigens capable of stimulating T-cell responses [11,12]. This was supported by a recent study showing that an mRNA vaccine induced *de novo* neoantigen-specific $CD8^+$ T-cells with multiyear persistence [13], suggesting that tailored immunotherapies, such as tumor-infiltrating lymphocyte (TIL) therapy, may hold promise for PDAC.

TIL therapy have demonstrated superior efficacy than ICB in the treatment of melanoma [14], leading to the FDA approval of the first T-cell-based immunotherapy to treat solid tumor, Lifileucel (AMTAGVI) [15]. This success is attributed to the broad T-cell specificities within the TIL product, which enable recognition of multiple tumor antigens [16,17], combined with their superior tumor-homing capacity [18,19]. Although PDAC is considered an "immunologically cold" tumor, growing evidence indicates that subsets of TILs with tumor-reactive and stem-like phenotypes exist within PDAC lesions [20–22]. Notably, a recent study demonstrated antitumor activity in a PDAC patient who achieved stable disease for over 1 year following TIL infusion [23], underscoring the feasibility and therapeutic potential of TIL therapy in this setting.

Recent innovations in TIL manufacturing, including optimized expansion protocols, cell engineering, and improved culture systems [24], have enabled the generation of highly functional TIL populations even from tumors with low baseline immune infiltration [25–27]. In this study, we report the use of IL-2/IL-15/IL-21-expanded TIL therapy in a PDAC patient under a compassionate use program, integrating genomic, transcriptomic, and T-cell receptor (TCR) profiling with functional immunological assays to investigate mechanisms underlying response and resistance.

Methods

TIL expansion

TILs were isolated from lung metastasis and expanded as previously reported [28]. Briefly, tumor tissue was mechanically dissected into fragments of approximately 8 mm^3 and cultured in a fully closed, GMP-compliant perfusion bioreactor platform developed for advanced therapy medicinal product manufacturing. Initial outgrowth (phase I) was performed in a 30-mm perfusion bioreactor, followed by large-scale expansion (phase II) in a 500-mm perfusion bioreactor at ZellWerk GmbH (Berlin, Germany).

Cultures were maintained in CellGro medium (CellGenix) supplemented with 10% human AB serum (ZKT Tübingen), 1% antibiotic–antimycotic solution (penicillin, streptomycin, amphotericin B; Sigma-Aldrich), and GMP-grade cytokines IL-2 (1000 IU/mL), IL-15 (180 IU/mL), and IL-21 (1 IU/mL) (Miltenyi Biotec GmbH, Germany). All reagents and consumables used during manufacturing were GMP-compliant.

At culture initiation, anti-CD3 antibody (clone OKT3, 30 ng/mL; Miltenyi Biotec) and gamma-irradiated (55 Gy) allogeneic peripheral blood mononuclear feeder cells ($1–2 \times 10^6$ cells pooled from four donors; ZKT Tübingen) were added once to support T-cell activation and expansion. Media perfusion and exchange were automatically regulated based on continuous monitoring of pH, hyperoxic pO_2, and temperature. Cell density, glucose consumption, and lactate production were routinely assessed throughout the expansion process. At harvest, cells were washed twice in 0.9% saline, formulated in 5% human albumin solution (Grifols), and transferred into infusion bags. The final product was transported to the clinical site under controlled ambient conditions (15–22°C).

Mutation profiling and neoepitope synthesis

Whole-exome sequencing (WES) was performed in genomic DNA isolated from tumor samples by CeGaT (Tübingen, Germany). The Agilent kit SureSelectXT Human All Exon V6 was used for library preparation prior to sequencing in a NovaSeq 6000 (Illumina, 2×100 bp). Post-sequencing data demultiplexing and trimming was performed with Illumina bcl2fastq (version 2.20) [29] and Skewer (version 0.2.2) [30] respectively. Sequencing data analysis was performed using the Illumina DRAGEN platform (version 4.2.4) [31]. RStudio was used to analyze the final data and generate figures using the R package *ggplot2*.

Mutations identified by WES were used to design 15-mer peptides with the mutated residue positioned centrally within the sequence as previously described [32]. For each neoepitope, the corresponding wild-type peptide was also synthesized, generating peptide pairs of mutant and wild-type sequences. These pairs were used in downstream immunological assays to compare T-cell recognition of mutant versus wild-type epitopes.

RNA sequencing

RNA isolated from fresh-frozen tumor tissue material was sent to CeGaT (Tübingen, Germany) for RNA sequencing. The SMARTer Stranded Total RNA Seq Kit v2-Pico Input (Takara) was used for library preparation prior to sequencing in a NovaSeq 6000 (Illumina, 2×100 bp Post-sequencing data demultiplexing and trimming was performed with Illumina bcl2fastq (version 2.20) [29] and Skewer (version 0.2.2) [30] respectively. Alignment to grch38 was performed using STAR (version 2.7.3) [33]. Differential expression analysis between groups was performed with DESeq2 (version 1.24.0) [34]. Gene ontogeny (GO) analysis was performed on differentially expressed genes [35]. The gene list containing genes with a $\log_2FC > 1.5$ and was used as input for the R package *clusterProfiler* (version 4.3.1.900) [36]. CIBERSORT was used to estimate the immune cell infiltration proportions by the standard LM22 signature matrix [37]. Principal component analysis (PCA) was performed using the R package *ggfortify*. Volcano plot was generated using the R package *EnhancedVolcano.*

Signature scores were computed by calculating the mean voom-normalized expression of predefined gene sets. T-cell–related programs included: TPEX (*TCF7, LEF1, IL7R, CCR7, CXCR5, SLAMF6*), Effector (*GZMB, GZMA, PRF1, NKG7, GNLY, IFNG, TBX21, EOMES, CX3CR1*), Pro-inflammatory (*CD8A, GZMA, GZMB, GZMH, GZMK, PRF1, NKG7*), Tumor-specific *(ENTPD1, ITGAE, PDCD1, CXCL13, TOX, HAVCR2, LAG3, TIGIT*), Exhaustion (*PDCD1, CTLA4, LAG3, HAVCR2, TIGIT, TOX, NR4A1, BATF, PRDM1*), and IFN-γ signature (*STAT1, IRF1, IDO1, CXCL9, CXCL10, HLA-A, HLA-B, HLA-C*). Tumor microenvironment signatures included cancer-associated fibroblasts (*ACTA2, TAGLN, FAP, COL1A1, PDGFRB, CXCL12*), myeloid cells (*CD68, CSF1R, MRC1, MERTK, SPP1, IL10*), and hypoxia (*HIF1A, CA9, SLC2A1, HK2, LDHA*). For each lesion, signature scores were obtained by averaging expression values across all genes in a given set. Data handling and visualization were performed in R using the packages *tidyverse, reshape2, ComplexHeatmap, pheatmap, circlize, RColorBrewer* and *ggplot2*.

TCR NGS

RNA samples isolated from the TIL products and tumor samples were sent to iRepertoire Inc (Huntsville, AL, USA) for TRB CDR3 next generation sequencing. TCRβ libraries were generated using one-step reverse transcription followed by purification and multiplex secondary amplification with Illumina adapter sequences. Libraries were sequenced on an Illumina MiSeq, and fastq files were processed on the iRepertoire webserver for V(D)J alignment. Mapped data were analyzed in the R package "*Immunarch*" to assess TCR diversity, overlap, spectratype, and clonotype tracking.

Histology

Specimens were fixed in 4% formalin, paraffin-embedded, sectioned at 4 μm, and stained with hematoxylin–eosin for histopathological assessment. Immunohistochemistry was performed as

previously described [32] to identify tumor-infiltrating infiltrating T-cells (CD3, CD4, CD8) and macrophages (CD68).

TILs' response to neoantigens and TCR identification

TILs were tested for immunoreactivity against mutated peptides as previsouly described [32,38]. Briefly, TILs were cultured with individual mutated peptide for 7 days at 37°C with 5% CO_2. Supernatants were collected and IFN-γ production was assessed using a standard ELISA kit following the manufacturer's guidelines (Mabtech, Stockholm, Sweden). Values from the negative control (medium) were subtracted from epitope (peptide)-specific responses and to reflect the net IFN-γ production from T-cell populations.

Antigen-reactive TILs were isolated as single cells by flow cytometric sorting following standard guidelines [17,39]. RNA from each cell was reverse-transcribed, and TCRα and TCRβ chains were amplified using nested RT-PCR with V- and C-region primers. Purified PCR products were sequenced by Sanger sequencing, enabling determination of paired CDR3α and CDR3β sequences at the single-cell level.

Killing assay

TILs' cytotoxicity against autologous tumor cell lines was determined as previously described [25]. Briefly, target cells comprising of autologous or control tumor cell lines were labelled with 100 μ of CiNa251CrO4 for 2 h. Target cells were then incubated with effector TILs at different effector:target ratios for 4 h at 37°C. Chromium-51 release in the supernatant was used to calculate TIL-mediated lysis of Cr-51–labeled target cells. K562 (ATCC no: CCL-243), Daudi B-lymphoma cell line (ATCC no: CRL-213) and autologous EBV-transformed B cell line served as controls.

TCGA database processing

RNA and WES data from the TCGA-PAAD cohort were analyzed using TIMER3 [40] and cBioPortal [41] respectively. We estimated the correlation between the expression of *ITGB2, C1QTNF3, CDK9, TMEM200C, FHOD1* and *ZZZ3* with CD8+ T-cells infiltration in PDAC using the Immune Infiltration Analysis Module with Spearman's correlation to adjust for purity [40]. Patient disease-free survival data was downloaded from cBioPortal and Kaplan-Meier plots with *P* values from a log rank test was determined based on somatic mutations on *TMEM200C, ITIH6, FHOD1, ITGB2, C1QTNF3, ADGRB1, OSBP2, CDK9, HDAC1* and *ZZZ3* [41] using the R package *survminer*.

Results

TIL product characteristics

The manufactured TIL products were tested as previously described [25]. Flow cytometric analysis demonstrated that the final products consisted predominantly of $CD3^+$ T cells (>97%), with marked enrichment of $CD3^+CD8^+$ subsets (>92%) and minimal $CD3^+CD4^+$ representation (<4%). Functional evaluation showed robust IFN-γ secretion following OKT3 stimulation and inducible CD107a expression upon PMA activation, confirming preserved cytotoxic capacity and overall product potency (Supplementary Figure).

Clinical course and treatment overview

The patient was a 39-year-old male diagnosed in February 2016 with metastatic pancreatic ductal adenocarcinoma (PDAC) involving bilateral lung, peritoneal, liver, and lymph node metastases. He received 16 cycles of mFOLFIRINOX (oxaliplatin 85 mg/m^2; irinotecan, 165 mg/m^2; leucovorin, 400 mg/m^2; and fluorouracil, 2400 mg/m^2, every 2 weeks), showing mixed radiologic response. Given the lack of sustained clinical benefit, the patient requested evaluation for TIL therapy and was admitted in January 2017. A large lung metastasis was surgically resected to manufacture an autologous TIL product while systemic FOLFIRINOX continued (Figure 1A).

The first infusion (0.5×10^9 TILs) was administered in May 2017 following low-dose conditioning with only cyclophosphamide (30 mg/kg) and a single low-dose IL-2 (60,000 IU/kg). This resulted in disease stabilization, prompting a second infusion (1.9×10^9 TILs) in June 2017 using a higher conditioning regimen (cyclophosphamide 60 mg/kg) and increased IL-2 dosing ($5 \times$ 60,000 IU/kg) to enhance cell persistence. Post-infusion, serum CA 19-9 levels declined (Figure 1B), and imaging revealed a mixed response: marked regression of one lung metastasis, stability of another, and persistence of the peritoneal lesion. In July 2017, all three lesions were excised for analysis by WES, RNA-seq and TRB NGS.

A third TIL infusion (1.2×10^9 TILs) was administered in August 2017 after lymphodepletion with cyclophosphamide (60 mg/kg) and high-dose IL-2 ($5 \times$ 600,000 IU/kg), aiming to further reduce host lymphocyte competition and boost *in vivo* TIL expansion. Cytokine analysis revealed transient elevations in IL-6, TNF-α, and soluble IL-2R following IL-2 administration (Figure 1C). Despite continued CA 19-9 decline, no additional clinical or radiologic benefit was observed, and imaging confirmed progressive disease. Three months later, new hepatic lesions developed, and the patient transitioned to palliative care. All three TIL infusions were well tolerated, with adverse events limited to transient fever and lymphopenia, the latter effectively managed with filgrastim.

Tumor genomic heterogeneity and mutational landscape impact on response

WES was performed on DNA from the lung metastasis used for TIL manufacturing (Harvest), a Regressing lung metastasis, a Stable lung metastasis, and a Progressing peritoneal metastasis (Figure 2A). The total non-synonymous somatic mutation burden across all lesions was low, ranging from a nonsynonymous tumor mutation burden (TMB) of 2.36 mutations/Mb at Harvest to 2.38, 3.17 and 2.91 mutations/Mb in the Regressing, Stable and Progressing lesions respectively, consistent with PDAC's typical low mutational load [42].

Analysis revealed pronounced inter-lesional heterogeneity at both the gene and mutation levels, with most alterations being unique to individual lesions (Figure 2B). The mutations were distributed across canonical pancreatic cancer genes, DNA damage repair genes, and other oncogenes but no chromatin remodeling genes. Notably, no KRAS mutations were detected in any lesion. Canonical PDAC driver mutations in *TP53* and *CDKN2A* were present only in post-TIL metastatic lesions and absent from the Harvest sample. In contrast, mutations in *RNF43, BRCA1/2, ATM, MSH2, NOV, SOX9, ERBB2* and *PIK3R3* were shared across all sites, consistent with a common clonal origin (Figure 2C). Of note, the regressing lesion harbored a higher number of somatic *TP53* mutations compared to the other lesions, potentially increasing its antigenic visibility to TIL therapy, whereas the progressing lesion's distinct mutational and immunosuppressive landscape may have hindered effective recognition and clearance.

We next examined private mutations exclusive to the progressing lesion. A total of 34 nonsynonymous variants, including missense, frameshift, and insertion/deletion events, were identified in genes linked to immune response and cancer metastasis (Figure 2D). Notable examples included *TMEM200C, ITIH6* and *FHOD1*—associated with invasion, immune escape, and extracellular matrix regulation predominantly expressed in stromal cells [43–45]; *ITGB2, C1QTNF3* and *ADGRB1*—involved in T-cell trafficking and immune modulation—expressed in TILs [46–48]; and *OSBP2, CDK9, HDAC1* and *ZZZ3*—implicated in proliferation, metastasis, epigenetic regulation, and tumor suppression—expressed in tumor cells [49–52].

Altogether, these mutations illustrate how stromal remodeling, immune modulation, and tumor-intrinsic programs may converge to dictate the extent of TIL infiltration and functionality, ultimately shaping therapeutic response in PDAC (Figure 2E). We therefore investigated the

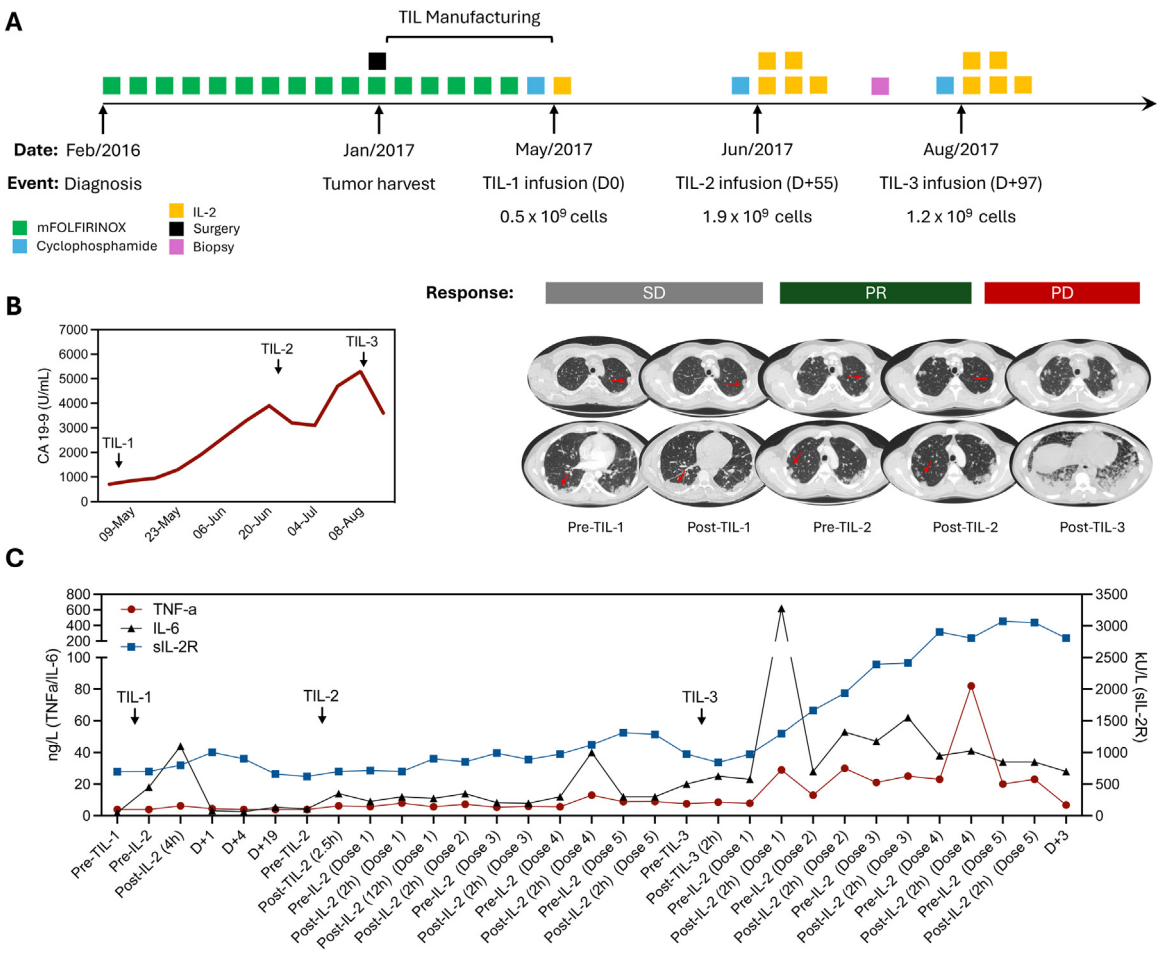

Fig. 1. Treatment timeline and clinical course during multiple TIL infusions in a patient with metastatic PDAC. (A) Chronological overview of clinical interventions and clinical course. Prior to TIL therapy, the patient received 16 cycles of mFOLFIRINOX (oxaliplatin 85 mg/m^2; irinotecan, 165 mg/m^2; leucovorin, 400 mg/m^2; and fluorouracil, 2400 mg/m^2, every 2 weeks). Lymphodepleting cyclophosphamide was administered before each TIL infusion (30 mg/kg before TIL-1; 60 mg/kg before TIL-2 and TIL-3). IL-2 support was administered post-infusion (TIL-1:1 × 60,000 IU/kg; TIL-2:5 × 60,000 IU/kg; TIL-3:5 × 600,000 IU/kg). TIL-1 (0.5 × 10^9 cells) was infused on day 0, TIL-2 (1.9 × 10^9 cells) on day +55, and TIL-3 (1.2 × 10^9 cells) on day +97. Lesion responses were assessed radiographically after each TIL infusion and classified as stable disease (SD), partial response (PR), and progressive disease (PD) respectively. (**B**) Serum cancer antigen 19-9 (CA 19-9) levels (U/mL) over the treatment course, with trends aligned to TIL infusion dates. **(C)** Plasma concentrations of TNF-α, IL-6 and soluble IL-2 receptor (sIL-2R) measured at multiple time points before and after TIL and IL-2 administration. Sampling points included pre- and post-IL-2 intervals (2–12 h) for up to five IL-2 doses per infusion, plus longitudinal follow-up at days +1, +4, +19, and +30 after each TIL administration. (Color version of figure is available online.)

relation between the expression of these genes and immune cell infiltration by analyzing the PAAD-TCGA dataset [53], as well as the impact of their mutation on patient outcome. Expression of *ITGB2, C1QTNF3, CDK9, TMEM200C, FHOD1*, and *ZZZ3* positively correlated with CD8+ T-cell infiltration (Figure 2F), supporting their role in orchestrating immune responses in PDAC. Moreover, patients with mutations in these genes exhibited shorter progression-free survival (Figure 2G), further underscoring their relevance as determinants of TIL responsiveness and potential biomarkers for adoptive cell therapy in PDAC.

T-cell diversity and immune activation in responding lesions

PCA of transcriptomic profiles revealed distinct clustering of each lesion, with the Regressing lesion positioned closest to the Stable lesion, while the Progressing and Harvest lesions showed the greatest divergence (Figure 3A). Immune deconvolution of RNA-seq data demonstrated striking differences in immune cell composition: the Regressing lesion was enriched for CD4$^+$ memory resting and CD8$^+$ T-cells, the Progressing lesion contained higher proportions of regulatory T-cells, M2 macrophages, and other immunosuppressive populations, and the Stable lesion displayed an intermediate profile (Figure 3B).

We identified differentially expressed genes between responding and non-responding lesions (Figure 3C), which clustered into signatures representing key processes linked to immunotherapy efficacy—including progenitor exhausted CD8$^+$ T-cells (Tpex) [54], effector function and pro-inflammatory activity [55], tumor-specificity [56], T-cell exhaustion and IFN-γ signaling [55,57]—as well as resistance programs such as cancer-associated fibroblast (CAF) or myeloid infiltration and hypoxia [58]. Stable and regressing lesions showed enrichment of transcriptional programs associated with activated and proliferating TILs (Figure 3D). Conversely, the progressing lesion exhibited upregulation of stromal- and myeloid-related genes, consistent with enhanced extracellular matrix remodeling, fibroblast activation, and vascular/stromal signaling. Together, these findings suggest that effective responses in PDAC are characterized by heightened proliferative immune activity coupled with suppression of stromal barriers that otherwise constrain TIL efficacy.

Gene Ontology analysis further highlighted lesion-specific programs, with “T-cell receptor complex” among the top enriched terms in the Regressing and Stable lesions, but absent in the Progressing lesion, which instead exhibited enrichment for structural and metabolic pathways unrelated to immune activation (Figure 3E). This suggested that different TIL infiltration patters could be related to lesion control. Analysis of TCR clonotypes showed that all the top 20 most frequent clonotypes in the Harvest sample (accounting for 26.8% of the repertoire) were also detected in the Stable and Regressing lesions after TIL therapy, representing 11.1% and 11.6% of their repertoires, respectively (Figure 3F). In contrast, only 11 clonotypes were

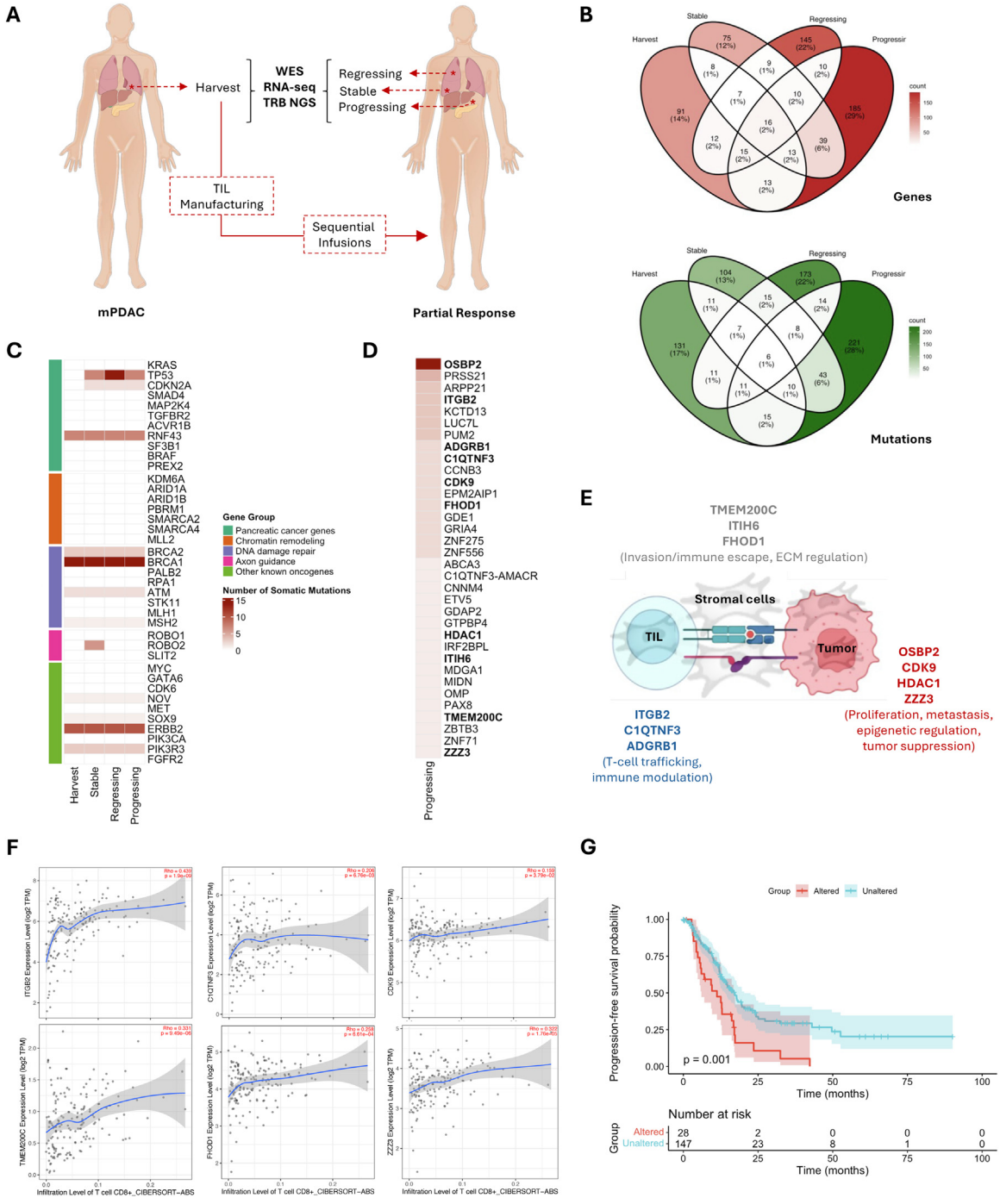

Fig. 2. Inter-tumoral heterogeneity impact on TIL infiltration and clinical response. (A) Schematic of sample collection and analytical workflow. Surgical resection material used for TIL manufacturing ("harvest") and biopsy samples collected after the second TIL infusion (stable lesion, regressing lesion, progressing lesion) underwent whole-exome sequencing (WES), bulk RNA sequencing (RNA-seq), and TCRβ next-generation sequencing (TRB NGS). (**B**) Venn diagrams showing the number of mutated genes (top) and total somatic mutations (bottom) unique or shared across lesions. (**C**) Mutation matrix panel depicting key genes and number of somatic mutations per gene. (**D**) Private nonsynonymous mutations found exclusively in the progressing lesion, with key genes involved in immune response, microenvironment modulation and tumor progression highlighted in bold. (**E**) Tumor microenvironment schematic depicting how the mutations may affect tumor control. (**F**) Scatter plots showing the positive correlation between the expression of *ITGB2, C1QTNF3, CDK9, TMEM200C, FHOD1* and *ZZZ3* with CD8+ T-cells infiltration in PDAC. Data from TIMER3.0 database (n = 178). (**G**) Kaplan–Meier survival curves of PDAC patients stratified by mutations in genes from panel **E**. Data from the TCGA PanCancer Atlas (n = 175). (Color version of figure is available online.)

identified in the Progressing lesion, where they occupied 9.7% of the repertoire due to overrepresentation of a few dominant clones (Figure 3G), resulting in reduced overall TCR diversity (Figure 3H). The high clonality and limited diversity in the Progressing lesion are consistent with impaired T-cell infiltration, in agreement with the transcriptomic findings. These data indicate that regressing and stable lesions were characterized by greater T-cell diversity and immune activation, whereas the progressing lesion exhibited restricted clonality and an immunosuppressive profile.

T-cell infiltration and TIL tracking

Considering the observed differences in mutation profiles, transcriptomics, and TCR characteristics across lesions, we next compared

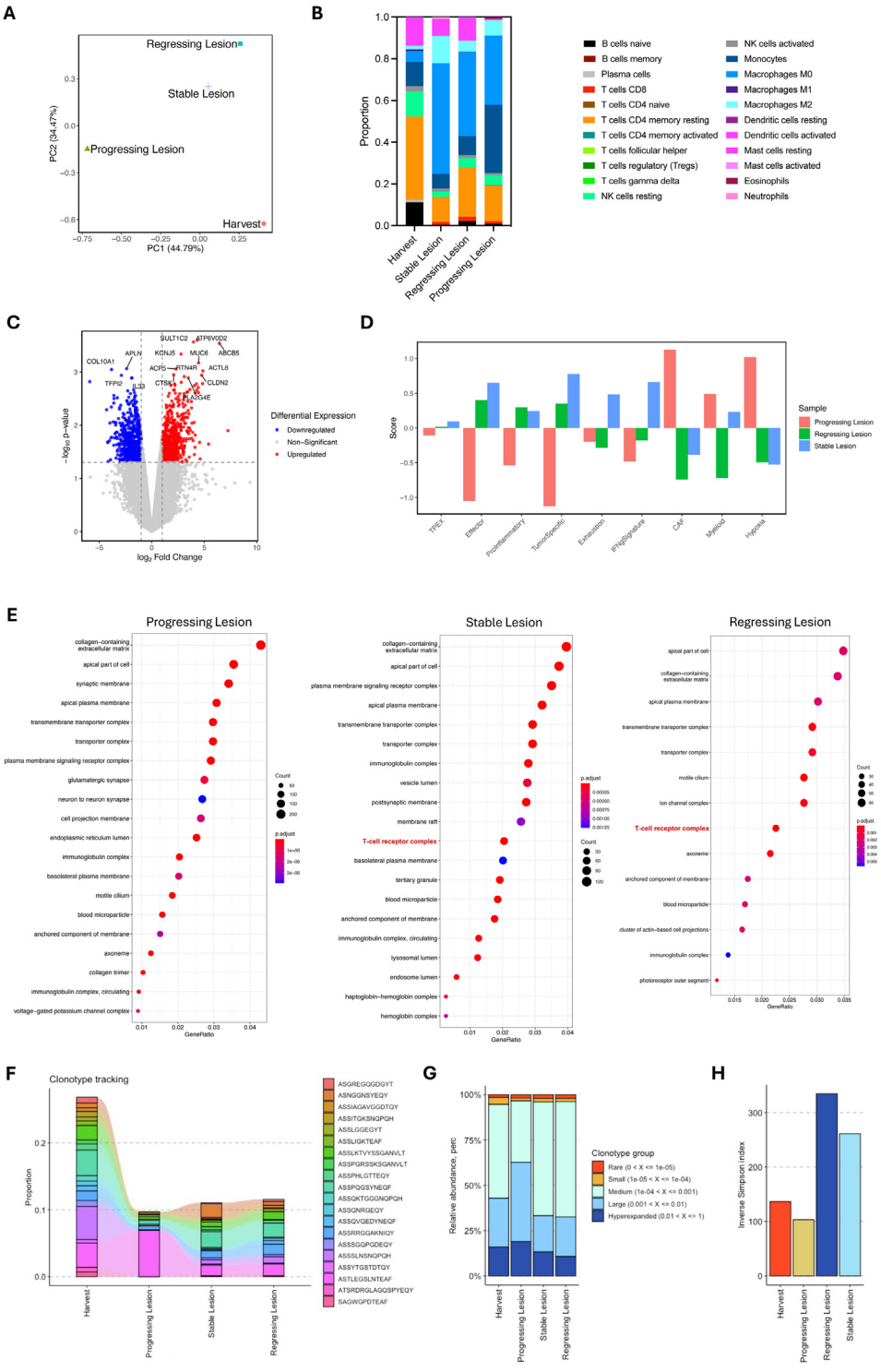

Fig. 3. Transcriptomic characterization of immune-mediated tumor control. (**A**) PCA of RNA-seq data showing separation of the harvest, stable, regressing, and progressing lesions. **(B)** Estimated immune cell type proportions inferred from bulk RNA-seq data using CIBERSORTx deconvolution, demonstrating differences in lymphoid, myeloid, and NK cell infiltration between lesions. (**C**) Volcano plot highlighting genes that are differentially expressed between responding and non-responding lesions. (**D**) Expression-based scores of differentially expressed genes grouped into predefined T-cell functional signatures and tumor microenvironment characteristics are shown for progressing, responding, and stable lesions. Each bar represents the relative enrichment of a given signature within an individual lesion. **(E)** Gene ontology enrichment analysis of differentially expressed genes for each lesion, showing enrichment in cellular component terms such as T-cell receptor complex, immunoglobulin complexes, plasma membrane–associated structures, and extracellular matrix organization. (**F**) Tracking of the 20 most frequent clones from the Harvest sample across the progressing, stable, and regressing lesions. (**G**) Distribution of clonotypes by homeostatic space, classified as hyperexpanded (1–100%), large (0.1–1%), medium (0.01–0.1%), or small (0–0.01%). (**H**) TRB diversity measured by the inverse Simpson's index. (Color version of figure is available online.)

the T-cell infiltrates and corresponding expanded TILs from each site. All lesions contained both CD4⁺ and CD8⁺ T-cells that could be successfully expanded into TIL products (Figure 4A). TCR CDR3 spectratyping of sorted CD4⁺ and CD8⁺ clonotypes revealed lesion-specific patterns: the Regressing lesion showed clonal dominance among CD4⁺ clonotypes carrying a TRBV12-4 gene segment, whereas the Stable lesion displayed dominance among CD8⁺ clonotypes with the same segment (Figure 4B). This indicates that different tumor lesions

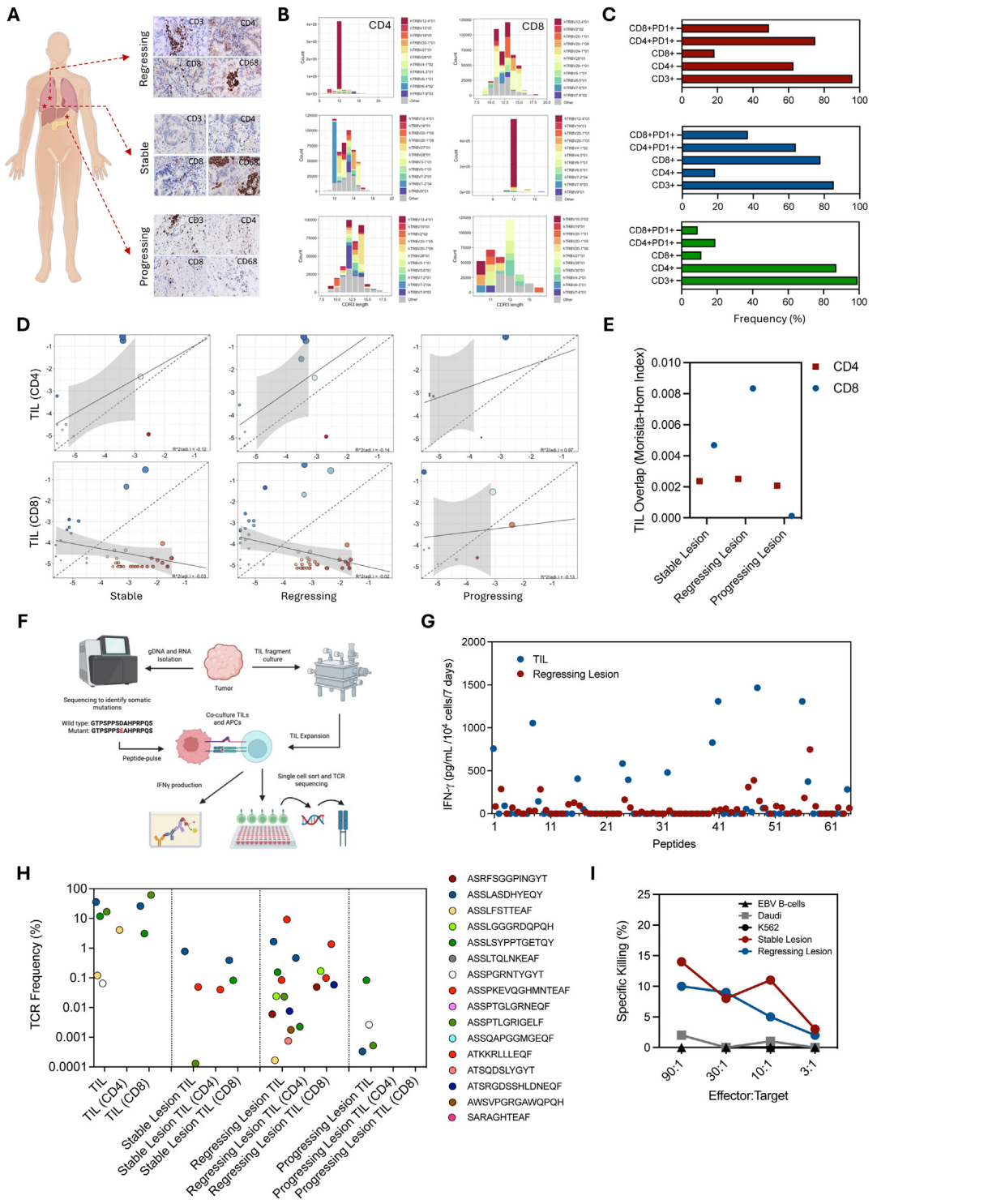

Fig. 4. Phenotypic, functional, and TCR repertoire analysis of lesion-derived TIL products. (A) Immunohistochemistry of tumor sections from regressing and stable lung metastases and a progressing peritoneal metastasis stained for CD3, CD4, CD8 (T-cell markers) and CD68 (macrophage marker). (**B**) CDR3 TRB spectratyping of sorted CD4$^+$ and CD8$^+$ T-cells from lesion-derived TIL products. **(C)** Flow cytometric quantification of CD3$^+$, CD4$^+$ and CD8$^+$ T-cells and PD-1 expression within bulk TIL products derived from each lesion. (**D**) Scatterplot comparing TRB repertoire overlap between sorted CD4$^+$ or CD8$^+$ TIL fractions and T-cells infiltrating the corresponding tumor lesions. **(E)** Morisita–Horn similarity index analysis of TRB repertoires in CD4$^+$ and CD8$^+$ TIL fractions from regressing, stable, and progressing lesions. **(F)** Experimental workflow: (i) WES of tumor lesions to identify nonsynonymous mutations, (ii) synthesis of corresponding peptides, (iii) *in vitro* stimulation of lesion-derived TILs, (iv) single-cell sorting and TCR identification, and (v) sequencing of bulk and sorted CD4$^+$/CD8$^+$ fractions to track mutation-reactive clonotypes. **(G)** IFN-γ production by peptide-stimulated TILs with predicted neoantigens. **(H)** Frequency of mutation-specific TCR clonotypes in each lesion-derived TIL product, stratified by CD4$^+$ and CD8$^+$ subsets. (**I**) Specific killing of tumor cell lines established from the Stable or Regressing metastatic lesion by the TIL product. Cr^{51}-labeled autologous tumor cell line or control tumor cell lines (targets) were incubated with tumor-infiltrating lymphocytes (effectors) at varying effector-to-target (E:T) ratios, and cytotoxic activity was calculated based on Cr^{51} release into the supernatant. Controls included the Daudi B-lymphoma cell line and autologous EBV-transformed B-cell line. (Color version of figure is available online.)

promoted the expansion of distinct T-cell subsets, with both CD4⁺ and CD8⁺ clonotypes likely recognizing a shared tumor antigen. These dominant clonotypes were associated with high PD-1 expression in the generated TIL products (Figure 4C), consistent with recent antigen encounter and sustained activation rather than terminal dysfunction. In contrast, the Progressing lesion lacked clonal dominance and exhibited low PD-1 expression (Figure 4B,C).

To confirm the origin of expanded TILs detected in the lesions, we performed a clonotype overlap analysis between the infused TIL product and the post-therapy lesions. CD8⁺ TIL-derived clonotypes showed greater persistence and infiltration than their CD4⁺ counterparts (Figure 4D), resulting in a higher degree of overlap with the tumor-infiltrating repertoire (Figure 4E). These findings suggest that CD8⁺ TIL-derived clonotypes played a central role in mediating tumor regression in PDAC.

TILs functional response

We next assessed the tumor reactivity of the infused TIL product by testing responses against mutated peptides and identifying the TRB sequences of tumor-specific T-cells (Figure 4F). TCR identification by Sanger sequencing of responder TILs enabled mapping of TRB CDR3 regions across all samples. Stimulation of the infused TIL product with 64 peptide pools elicited responses against 18 pools, consistent with a polyclonal T-cell repertoire characteristic of TIL products (Figure 4G). A comparable pattern was observed in the TILs expanded from the Regressing lesion post-therapy, confirming that tumor-specific T-cells were retained and contributed to local tumor control.

Tracking of tumor-specific TCR clonotypes revealed that, despite the polyfunctional profile of the Harvest-derived TIL product, the Regressing lesion contained the highest presence of multiple tumor-specific TCRs, particularly within the CD8⁺ compartment (Figure 4H). In contrast, only a few tumor-specific clonotypes were detected in the Progressing lesion. Functionally, the infused TIL product specifically lysed autologous tumor cell lines derived from the Stable and Regressing lesions in a dose-dependent manner (Figure 4I), while sparing the autologous EBV-transformed B-cell line. Collectively, these results demonstrate that both the infused TIL product and the TILs expanded from the Regressing lesion mounted broad, mutation-specific responses, and that responding lesions were selectively enriched for tumor-specific T-cells with cytolytic capacity.

Discussion

This case report extends the application of TIL therapy beyond traditionally immunologically “hot” tumors such as melanoma and lung cancer. The approach was feasible and did not raise unexpected safety concerns despite the use of multiple TIL and IL-2 administrations, with most adverse events consisting of anticipated cytopenias related to the reduced-intensity lymphodepleting chemotherapy. Notably, we showed genomic, transcriptomic and functional correlates between responding and non-responding metastatic lesions, demonstrating the association between multiple target recognition and TIL infiltration with tumor control in PDAC.

Although relatively low doses of TIL were administered in this case ($0.5–2.1 \times 10^9$ cells) compared with other protocols (median dose of 21.1×10^9 cells) [15], the patient progressed from stable disease after the first infusion to a partial response after the second. This finding suggests that multiple TIL administrations may enhance pharmacokinetic and pharmacodynamic profiles, a concept also associated with improved outcomes in CAR-T therapy [59]. We have reported similar favorable results with repeated TIL administrations in a prostate [25,27] and glioblastoma [26] patient, suggesting that this approach may enhance TIL responses in immunologically cold tumors.

PDAC is characterized by a low TMB [42], a feature consistently associated with poor responsiveness to immunotherapy [11]. Although the overall number of mutations is relatively low, these alterations are predominantly clonal, with *KRAS* mutations present in approximately 90% of cases [60] and linked to poor survival [61,62]. Targeted strategies such as *KRAS-G12C* inhibitors (Sotorasib and Adagrasib) [63] or *KRAS-G12V* neoantigen-specific TCR-T cells [64] represent promising therapeutic options but are limited to patients carrying specific mutations and HLA alleles. In contrast, TIL therapy is mutation-agnostic, offering broader applicability across patients regardless of their genomic background. In the present case, although a canonical *KRAS* driver mutation was absent, alterations in *TP53, CDKN2A* and *RNF43* were identified. Although these genes drive PDAC progression and are often linked to poor therapeutic response, clinical experience indicates that only a minority of patients can benefit from targeting such mutations, due to the lack of available drugs and the undruggable nature of many driver genes [65]. Here, we demonstrated that IL-2/IL-15/IL-21-expanded TILs exert antitumor activity through recognition of multiple tumor-derived antigens and possess intrinsic tumor-homing capacity, enabling effective immune targeting even when driver mutations are undruggable or lack available therapies.

Previous studies have highlighted the heterogeneity of the PDAC tumor microenvironment across metastatic sites, reflecting adaptation to local niches and enrichment of oncogenic programs such as *TP53* activation [66]. Although *TP53* mutations were not detected in the tumor material harvested for TIL manufacturing, varying levels of somatic mutations emerged in metastatic lesions post-treatment. *TP53* dysfunction is known to reshape the TME by impairing antigen presentation, altering cytokine signaling, and fostering an immunosuppressive milieu that facilitates tumor progression [67]. The Regressing lesion harbored a higher number of TP53 mutations, potentially broadening the repertoire of immunogenic peptides available for TIL recognition and contributing to the observed therapeutic response, as previously described [68,69].

Our findings highlight that private mutations in the progressing lesion were not random but enriched in pathways central to tumor–immune interactions, stromal remodeling, and tumor-intrinsic survival programs. Genes such as *TMEM200C, ITIH6* and *FHOD1*, predominantly expressed in stromal compartments, suggest that alterations in the extracellular matrix and tissue architecture may directly influence T-cell infiltration by creating either permissive or restrictive niches [43–45]. Similarly, mutations in *ITGB2, C1QTNF3, and ADGRB1*, which are expressed in TILs and regulate trafficking and immune communication, point to a model where tumor evolution actively shapes immune accessibility [46–48]. In parallel, tumor-intrinsic alterations in *OSBP2, CDK9, HDAC1* and *ZZZ3* converge on proliferation, epigenetic regulation, and stress resistance, representing another layer of adaptation that could undermine T-cell recognition and effector function [49–52].

Responding lesions were enriched for transcriptional programs of activated and proliferating TILs, whereas the progressing lesion upregulated stromal and myeloid genes linked to extracellular matrix remodeling and fibroblast activation. These findings confirm previous observations in melanoma [69] and suggest that TIL therapy outcomes are shaped not only by the intrinsic properties of infused lymphocytes but also by the tumor’s mutational and stromal context [70,71]. The correlation of *ITGB2, C1QTNF3, CDK9, TMEM200C, FHOD1* and *ZZZ3* expression with CD8+ T-cell infiltration together with the association of their mutations with shorter progression-free survival, underscores their potential as biomarkers of immune responsiveness in PDAC.

CAR-T cell have been evaluated in PDAC by targeting highly expressed single antigens such as CD133 [72], EGFR [73], HER2 [74] and MSLN [75–77], yet most patients experienced only short-term stable disease or no clinical benefit. These poor outcomes are

attributed to CAR-T exhaustion [77], limited infiltration into the tumor and the restricted repertoire of targetable antigens [78], which are often heterogeneously expressed. In contrast, TIL therapy offers key advantages, including superior tumor-homing capacity due to their intratumoral origin and the ability to recognize a broad array of tumor antigens [16–19]. This study demonstrates that effective TIL infiltration, coupled with recognition of a wide spectrum of tumor antigens, is associated with tumor control.

Despite its conceptual advantages, TIL therapy faces several important challenges that may limit broader implementation. First, TIL manufacturing requires sufficient tumor tissue and viable lymphocyte outgrowth, which can be particularly difficult in immunologically "cold" tumors such as PDAC [79]. Second, the manufacturing process remains labor-intensive and time-sensitive, potentially restricting scalability and rapid clinical deployment [80]. Third, intratumoral heterogeneity and dynamic immune evasion mechanisms, including antigen loss or T-cell dysfunction, may compromise durable responses [23,81]. Finally, patient selection, optimal conditioning regimens, and identification of predictive biomarkers remain areas requiring further investigation [80,81]. Addressing these biological and logistical barriers will be critical for expanding the clinical applicability of TIL therapy beyond selected cases.

This case highlights the feasibility and safety of IL-2/IL-15/IL-21-expanded TIL therapy in PDAC, where repeated low-dose infusions achieved tumor infiltration, multi-antigen recognition, and clinical benefit. The findings underscore that TIL efficacy is shaped by both lymphocyte properties and the mutational–stromal context, supporting further development of TIL therapy as a mutation-agnostic approach for this genomically heterogeneous disease.

Data availability

Sequencing data are available under accession numbers GSE306970, GSE306971 and GSE306972. Other raw data are available from the corresponding author upon request.

Ethics approval and patient consent

Ethics committee approval was not required, as the treatment was administered under single-patient compassionate use regulations in Germany, which are not subject to ethics committee oversight. The patient provided written informed consent prior to treatment, including consent for data collection and publication.

Funding

No funding was received.

Declaration of competing interest

L.C.M.A is an employee of CuraCell Holding AB. J.K. and E.J. are consultants of CuraCell Holding AB. E. S., D. G. and H. H. are employees of Zellwerk GmbH. The authors declare that they have no other competing interests.

Acknowledgments

The authors thank Claudia Wahle for her excellent work in tumor and T-cell culturing, and the Champalimaud Foundation for supporting the multi-omics and flow cytometry analyses.

Supplementary materials

Supplementary material associated with this article can be found in the online version at doi:10.1016/j.jcyt.2026.102141.

Article History:

Received 6 January 2026
Accepted 2 March 2026

References

[1] Stoop TF, Javed AA, Oba A, Koerkamp BG, Seufferlein T, Wilmink JW, et al. Pancreatic cancer. Lancet 2025;405:1182–202.
[2] Halbrook CJ, Lyssiotis CA, Pasca di Magliano M, Maitra A. Pancreatic cancer: advances and challenges. Cell 2023;186:1729–54.
[3] Hsu S-K, Jadhao M, Liao W-T, Chang W-T, Hung C-T, Chiu C-C. Culprits of PDAC resistance to gemcitabine and immune checkpoint inhibitor: tumour microenvironment components. Front Mol Biosci 2022;9:1–12.
[4] Ju Y, Xu D, Liao M, Sun Y, Bao W, Yao F, et al. Barriers and opportunities in pancreatic cancer immunotherapy. NPJ Precis Oncol 2024;8:199.
[5] Royal RE, Levy C, Turner K, Mathur A, Hughes M, Kammula US, et al. Phase 2 trial of single agent ipilimumab (Anti-CTLA-4) for locally advanced or metastatic pancreatic adenocarcinoma. J Immunother 2010;33:828–33.
[6] Brahmer JR, Tykodi SS, Chow LQM, Hwu W-J, Topalian SL, Hwu P, et al. Safety and activity of anti–PD-L1 antibody in patients with advanced cancer. N Engl J Med 2012;366:2455–65.
[7] O'Reilly EM, Oh D-Y, Dhani N, Renouf DJ, Lee MA, Sun W, et al. Durvalumab with or without tremelimumab for patients with metastatic pancreatic ductal adenocarcinoma. JAMA Oncol 2019;5:1431.
[8] Hecht JR, Lonardi S, Bendell J, Sim H-W, Macarulla T, Lopez CD, et al. Randomized phase III study of FOLFOX alone or with pegilodecakin as second-line therapy in patients with metastatic pancreatic cancer that progressed after gemcitabine (SEQUOIA). J Clin Oncol 2021;39:1108–18.
[9] Hewitt DB, Nissen N, Hatoum H, Musher B, Seng J, Coveler AL, et al. A phase 3 randomized clinical trial of chemotherapy with or without algenpantucel-L (Hyper-Acute-pancreas) immunotherapy in subjects with borderline resectable or locally advanced unresectable pancreatic cancer. Ann Surg 2022;275:45–53.
[10] Yarchoan M, Hopkins A, Jaffee EM. Tumor mutational burden and response rate to PD-1 inhibition. N Engl J Med 2017;377:2500–1.
[11] Łuksza M, Sethna ZM, Rojas LA, Lihm J, Bravi B, Elhanati Y, et al. Neoantigen quality predicts immunoediting in survivors of pancreatic cancer. Nature 2022;606:389–95.
[12] Balachandran VP, Łuksza M, Zhao JN, Makarov V, Moral JA, Remark R, et al. Identification of unique neoantigen qualities in long-term survivors of pancreatic cancer. Nature 2017;551:512–6.
[13] Sethna Z, Guasp P, Reiche C, Milighetti M, Ceglia N, Patterson E, et al. RNA neoantigen vaccines prime long-lived CD8+ T cells in pancreatic cancer. Nature 2025;639:1042–51.
[14] Rohaan MW, Borch TH, van den Berg JH, Met Ö, Kessels R, Geukes Foppen MH, et al. Tumor-infiltrating lymphocyte therapy or ipilimumab in advanced melanoma. N Engl J Med 2022;387:2113–25.
[15] Keam SJ. Lifileucel: first approval. Mol Diagn Ther 2024;28:339–44.
[16] Pétremand R, Chiffelle J, Bobisse S, Perez MAS, Schmidt J, Arnaud M, et al. Identification of clinically relevant T cell receptors for personalized T cell therapy using combinatorial algorithms. Nat Biotechnol 2025;43:323–8.
[17] Zacharakis N, Chinnasamy H, Black M, Xu H, Lu YC, Zheng Z, et al. Immune recognition of somatic mutations leading to complete durable regression in metastatic breast cancer. Nat Med 2018;24:724–30.
[18] Mrass P, Takano H, Ng LG, Daxini S, Lasaro MO, Iparraguirre A, et al. Random migration precedes stable target cell interactions of tumor-infiltrating T cells. J Exp Med 2006;203:2749–61.
[19] Mohammadi Y, Khorramdelazad H, Soleimanifar N, Badalzadeh M, Nicknam MH, Kardar GA. The critical role of homing in TIL therapy success: from biology to clinical application. Crit Rev Oncol Hematol 2025:1–19. 104930.
[20] Ino Y, Yamazaki-Itoh R, Shimada K, Iwasaki M, Kosuge T, Kanai Y, et al. Immune cell infiltration as an indicator of the immune microenvironment of pancreatic cancer. Br J Cancer 2013;108:914–23.
[21] Gorchs L, Fernández-Moro C, Asplund E, Oosthoek M, Solders M, Ghorbani P, et al. Exhausted tumor-infiltrating CD39+CD103+ CD8+ T cells unveil potential for increased survival in human pancreatic cancer. Cancer Res Commun 2024;4:460–74.
[22] Carstens JL, Correa de Sampaio P, Yang D, Barua S, Wang H, Rao A, et al. Spatial computation of intratumoral T cells correlates with survival of patients with pancreatic cancer. Nat Commun 2017;8:15095.
[23] Amaria R, Knisely A, Vining D, Kopetz S, Overman MJ, Javle M, et al. Efficacy and safety of autologous tumor-infiltrating lymphocytes in recurrent or refractory ovarian cancer, colorectal cancer, and pancreatic ductal adenocarcinoma. J Immunother Cancer 2024;12:1–11.
[24] Amaria RN, Komanduri KV, Schoenfeld AJ, Ramsingh G, Burga RA, Jagasia MH. Entering a new era of tumor-infiltrating lymphocyte cell therapy innovation. Cytotherapy 2025;27:864–73.
[25] Karbach J, Kiselicki D, Brand K, Wahle C, Sinelnikov E, Gustavus D, et al. Tumor-infiltrating lymphocytes mediate complete and durable remission in a patient with NY-ESO-1 expressing prostate cancer. J Immunother Cancer 2023;11:e005847.
[26] Arruda LCM, Karbach J, Kiselicki D, Altmannsberger HM, Sinelnikov E, Gustavus D, et al. Tumor-infiltrating lymphocytes-derived CD8+ clonotypes infiltrate the tumor tissue and mediate tumor regression in glioblastoma. OncoImmunology 2025;14(1):1–16. https://doi.org/10.1080/2162402X.2025.2559784. 2559784.

[27] Arruda LCM, Karbach J, Kiselicki D, Brand K, Wahle C, Sinelnikov E, et al. Serial TIL infusions and PD-1 blockade drive long-term clonal persistence in prostate cancer. Front Oncol 2025;15:1693912.
[28] Albrecht HC, Gustavus D, Schwanemann J, Dammermann W, Lippek F, Weylandt K-H, et al. Generation of colon cancer–derived tumor-infiltrating T cells (TILs) for adoptive cell therapy. Cytotherapy 2023;25:537–47.
[29] Cock PJA, Fields CJ, Goto N, Heuer ML, Rice PM. The sanger FASTQ file format for sequences with quality scores, and the Solexa/Illumina FASTQ variants. Nucleic Acids Res 2010;38:1767–71.
[30] Jiang H, Lei R, Ding S-W, Zhu S. Skewer: a fast and accurate adapter trimmer for next-generation sequencing paired-end reads. BMC Bioinformatics 2014;15:182.
[31] Danecek P, Auton A, Abecasis G, Albers CA, Banks E, DePristo MA, et al. The variant call format and VCFtools. Bioinformatics 2011;27:2156–8.
[32] Meng Q, Valentini D, Rao M, Moro CF, Paraschoudi G, Jäger E, et al. Neoepitope targets of tumour-infiltrating lymphocytes from patients with pancreatic cancer. Br J Cancer 2019;120:97–108.
[33] Dobin A, Davis CA, Schlesinger F, Drenkow J, Zaleski C, Jha S, et al. STAR: ultrafast universal RNA-seq aligner. Bioinformatics 2013;29:15–21.
[34] Love MI, Huber W, Anders S. Moderated estimation of fold change and dispersion for RNA-seq data with DESeq2. Genome Biol 2014;15:550.
[35] Ashburner M, Ball CA, Blake JA, Botstein D, Butler H, Cherry JM, et al. Gene ontology: tool for the unification of biology. Nat Genet 2000;25:25–9.
[36] Wu T, Hu E, Xu S, Chen M, Guo P, Dai Z, et al. clusterProfiler 4.0: a universal enrichment tool for interpreting omics data. Innovation 2021;2:100141.
[37] Chen B, Khodadoust MS, Liu CL, Newman AM, Alizadeh AA. Profiling tumor infiltrating immune cells with CIBERSORT. Methods Mol Biol 2018;1711:243–59.
[38] Valentini D, Rao M, Meng Q, von Landenberg A, Bartek J, Sinclair G, et al. Identification of neoepitopes recognized by tumor-infiltrating lymphocytes (TILs) from patients with glioma. Oncotarget 2018;9:19469–80.
[39] Han A, Glanville J, Hansmann L, Davis MM. Linking T-cell receptor sequence to functional phenotype at the single-cell level. Nat Biotechnol 2014;32:684–92.
[40] Cui H, Zhao G, Lu Y, Zuo S, Duan D, Luo X, et al. TIMER3: an enhanced resource for tumor immune analysis. Nucleic Acids Res 2025;53:W534–41.
[41] Gao J, Aksoy BA, Dogrusoz U, Dresdner G, Gross B, Sumer SO, et al. Integrative analysis of complex cancer genomics and clinical profiles using the cBioPortal. Sci Signal 2013;6:1–19.
[42] Waddell N, Pajic M, Patch A-M, Chang DK, Kassahn KS, Bailey P, et al. Whole genomes redefine the mutational landscape of pancreatic cancer. Nature 2015;518:495–501.
[43] Yang Y, Kang Z, Cai J, Jia S, Fan S, Zhu H. Role of FHOD1 in tumor cells and tumor immune microenvironment. Front Immunol 2025;16:1–9.
[44] Liu J, Cao F, Li X, Zhang L, Liu Z, Li X, et al. ITIH5, a p53-responsive gene, inhibits the growth and metastasis of melanoma cells by downregulating the transcriptional activity of KLF4. Cell Death Dis 2021;12:438.
[45] Fang F, Zhang T, Lei H, Shen X. TMEM200A is a potential prognostic biomarker and correlated with immune infiltrates in gastric cancer. Peer J 2023;11:e15613.
[46] Islam S, Kitagawa T, Baron B, Abiko Y, Chiba I, Kuramitsu Y. ITGA2, LAMB3, and LAMC2 may be the potential therapeutic targets in pancreatic ductal adenocarcinoma: an integrated bioinformatics analysis. Sci Rep 2021;11:10563.
[47] Micallef P, Vujičić M, Wu Y, Peris E, Wang Y, Chanclón B, et al. C1QTNF3 is upregulated during subcutaneous adipose tissue remodeling and stimulates macrophage chemotaxis and M1-like polarization. Front Immunol 2022;13:914956.
[48] Aust G, Zhu D, Van Meir EG, Xu L, Adhesion G. Protein-coupled Receptors. In: Langenhan T, Schöneberg T, eds. Handbook of Experimental Pharmacology, 234, Cham: Springer; 2016 https://doi.org/10.1007/978-3-319-41523-9_17.
[49] Sheng H, Zheng F, Lan T, Chen H, Xu C, Wang S, et al. YEATS2 regulates the activation of TAK1/NF-κB pathway and is critical for pancreatic ductal adenocarcinoma cell survival. Cell Biol Toxicol 2023;39:1–16.
[50] Zhang W, Ge L, Zhang Y, Zhang Z, Zhang W, Song F, et al. Targeted intervention of tumor microenvironment with HDAC inhibitors and their combination therapy strategies. Eur J Med Res 2025;30:69.
[51] Kretz A-L, Schaum M, Richter J, Kitzig EF, Engler CC, Leithäuser F, et al. CDK9 is a prognostic marker and therapeutic target in pancreatic cancer. Tumor Biol 2017;39:1–12.
[52] Huang S, Zhang X, Luo K, Jiang L, Jiang J, Li R. Oxysterol-binding protein 2 promotes pancreatic ductal adenocarcinoma progression through epithelial-mesenchymal transition. Front Oncol 2022;11:1–13.
[53] Raphael BJ, Hruban RH, Aguirre AJ, Moffitt RA, Yeh JJ, Stewart C, et al. Integrated genomic characterization of pancreatic ductal adenocarcinoma. Cancer Cell 2017;32:185–203.e13.
[54] Rahim MK, Okholm TLH, Jones KB, McCarthy EE, Liu CC, Yee JL, et al. Dynamic CD8 + T cell responses to cancer immunotherapy in human regional lymph nodes are disrupted in metastatic lymph nodes. Cell 2023;186:1127–1143.e18.
[55] Litchfield K, Reading JL, Puttick C, Thakkar K, Abbosh C, Bentham R, et al. Meta-analysis of tumor- and T cell-intrinsic mechanisms of sensitization to checkpoint inhibition. Cell 2021;184:596–614.e14.
[56] Duhen T, Duhen R, Montler R, Moses J, Moudgil T, de Miranda NF, et al. Co-expression of CD39 and CD103 identifies tumor-reactive CD8 T cells in human solid tumors. Nat Commun 2018;9:2724.
[57] Zheng L, Qin S, Si W, Wang A, Xing B, Gao R, et al. Pan-cancer single-cell landscape of tumor-infiltrating T cells. Science 2021;374:abe6474.
[58] Chen Q, Sun T, Jiang C. Recent advancements in nanomedicine for 'cold' tumor immunotherapy. Nanomicro Lett 2021;13:92.
[59] Kirouac DC, Zmurchok C, Morris D. Making drugs from T cells: the quantitative pharmacology of engineered T cell therapeutics. NPJ Syst Biol Appl 2024;10:31.
[60] Witkiewicz AK, McMillan EA, Balaji U, Baek G, Lin W-C, Mansour J, et al. Whole-exome sequencing of pancreatic cancer defines genetic diversity and therapeutic targets. Nat Commun 2015;6:6744.
[61] Shin SH, Kim SC, Hong S-M, Kim YH, Song K-B, Park K-M, et al. Genetic alterations of K-ras, p53, c-erbB-2, and DPC4 in pancreatic ductal adenocarcinoma and their correlation with patient survival. Pancreas 2013;42:216–22.
[62] Kim ST, Lim DH, Jang K-T, Lim T, Lee J, Choi Y-L, et al. Impact of *KRAS* mutations on clinical outcomes in pancreatic cancer patients treated with first-line gemcitabine-based chemotherapy. Mol Cancer Ther 2011;10:1993–9.
[63] Kwan AK, Piazza GA, Keeton AB, Leite CA. The path to the clinic: a comprehensive review on direct KRASG12C inhibitors. J Exp Clin Cancer Res 2022;41:27.
[64] Lu D, Chen Y, Jiang M, Wang J, Li Y, Ma K, et al. KRAS G12V neoantigen specific T cell receptor for adoptive T cell therapy against tumors. Nat Commun 2023;14:6389.
[65] Swayden M, Iovanna J, Soubeyran P. Pancreatic cancer chemo-resistance is driven by tumor phenotype rather than tumor genotype. Heliyon 2018;4:e01055.
[66] Khaliq AM, Rajamohan M, Saeed O, Mansouri K, Adil A, Zhang C, et al. Spatial transcriptomic analysis of primary and metastatic pancreatic cancers highlights tumor microenvironmental heterogeneity. Nat Genet 2024;56:2455–65.
[67] Shi Y, Ren X, Cao S, Chen X, Yuan B, Brasil da Costa FH, et al. *TP53* gain-of-function mutation modulates the immunosuppressive microenvironment in non-HPV-associated oral squamous cell carcinoma. J Immunother Cancer 2023;11:e006666.
[68] Levi ST, Copeland AR, Nah S, Crystal JS, Ivey GD, Lalani A, et al. Neoantigen identification and response to adoptive cell transfer in anti–PD-1 naïve and experienced patients with metastatic melanoma. Clin Cancer Res 2022;28:3042–52.
[69] Lauss M, Donia M, Harbst K, Andersen R, Mitra S, Rosengren F, et al. Mutational and putative neoantigen load predict clinical benefit of adoptive T cell therapy in melanoma. Nat Commun 2017;8:1738.
[70] Liu X, Baer JM, Stone ML, Knolhoff BL, Hogg GD, Turner MC, et al. Stromal reprogramming overcomes resistance to RAS-MAPK inhibition to improve pancreas cancer responses to cytotoxic and immune therapy. Sci Transl Med 2024;16:eado2402.
[71] Ullman NA, Burchard PR, Dunne RF, Linehan DC. Immunologic strategies in pancreatic cancer: making *cold* tumors *hot*. J Clin Oncol 2022;40:2789–805.
[72] Wang Y, Chen M, Wu Z, Tong C, Dai H, Guo Y, et al. CD133-directed CAR T cells for advanced metastasis malignancies: a phase I trial. Oncoimmunology 2018;7:e1440169.
[73] Liu Y, Guo Y, Wu Z, Feng K, Tong C, Wang Y, et al. Anti-EGFR chimeric antigen receptor-modified T cells in metastatic pancreatic carcinoma: a phase I clinical trial. Cytotherapy 2020;22:573–80.
[74] Feng K, Liu Y, Guo Y, Qiu J, Wu Z, Dai H, et al. Phase I study of chimeric antigen receptor modified T cells in treating HER2-positive advanced biliary tract cancers and pancreatic cancers. Protein Cell 2018;9:838–47.
[75] Haas AR, Tanyi JL, O'Hara MH, Gladney WL, Lacey SF, Torigian DA, et al. Phase I study of lentiviral-transduced chimeric antigen receptor-modified T cells recognizing mesothelin in advanced solid cancers. Mol Ther 2019;27:1919–29.
[76] Beatty GL, O'Hara MH, Lacey SF, Torigian DA, Nazimuddin F, Chen F, et al. Activity of mesothelin-specific chimeric antigen receptor T cells against pancreatic carcinoma metastases in a phase 1 trial. Gastroenterology 2018;155:29–32.
[77] Aznar MA, Good CR, Barber-Rotenberg JS, Agarwal S, Wilson W, Watts A, et al. Clinical and molecular dissection of CAR T cell resistance in pancreatic cancer. Cell Rep Med 2025;6:102301.
[78] Du B, Qin J, Lin B, Zhang J, Li D, Liu M. CAR-T therapy in solid tumors. Cancer Cell 2025;43:665–79.
[79] Coukos G, Donia M, Gastman BR, Goff SL, Gros A, Harari A, et al. The science of tumor-infiltrating lymphocytes (TIL): perspectives from the SITC Surgery Committee. J Immunother Cancer 2025;13:e013420.
[80] Turcotte S, Donia M, Gastman B, Besser M, Brown R, Coukos G, et al. Art of TIL immunotherapy: SITC's perspective on demystifying a complex treatment. J Immunother Cancer 2025;13:1–16. e010207.
[81] Navarro Rodrigo B, Ortiz Miranda Y, Corria-Osorio J, Coukos G, Harari A. Immune correlates and mechanisms of TIL therapy efficacy: current insights and knowledge gaps. Trends Cancer 2025;11:993–1004.